

# THE EFFECT OF RELATIVE DENSITY, GRANULARITY AND SIZE OF GEOGRID APERTURES ON THE SHEAR STRENGTH OF THE SOIL/GEOGRID INTERFACE

Ali LAKIROUHANI<sup>1</sup>, Mojgan ABBASIAN<sup>1</sup>,  
 Jurgis MEDZVIECKAS<sup>2✉</sup>, Romualdas KLIUKAS<sup>3</sup>

<sup>1</sup>Department of Civil Engineering, Faculty of Engineering, University of Zanjan, Zanjan, Iran

<sup>2</sup>Department of Reinforced Concrete Structures and Geotechnics, Vilnius Gediminas Technical University, Saulėtekio al. 11, 10223 Vilnius, Lithuania

<sup>3</sup>Department of Applied Mechanics, Vilnius Gediminas Technical University, Saulėtekio al. 11, 10223 Vilnius, Lithuania

## Article History:

- received 20 February 2024
- accepted 25 July 2024

**Abstract.** The increasing use of geogrid in various geotechnical projects has made the evaluation of the shear behavior of soil reinforced with geogrid become particularly important. In this article, a series of large-scale direct shear tests have been performed on sand and gravel samples reinforced with geogrid. The purpose of the experiments was to investigate the impact of the geogrid mesh size and the relative density of the samples on the shear strength coefficient of the interface between soil and geogrid. In this study, 5 geogrids with different mesh sizes and one type of geotextile were used. According to the results, the average shear strength coefficient of sand and gravel samples reinforced with geogrid for different normal stresses and different relative densities was obtained between 0.72 and 0.94. As the relative density increases, the interface shear strength coefficient decreases, this means that the denser the sand, the more the shear strength of the sand/geogrid interface decreases. Based on the results, it was found that the contribution of particle interlocking in the shear resistance of the sand/geogrid interface is particularly important, so that the shear resistance coefficient of the interface increases with the increase in the size of the geogrid mesh.

**Keywords:** shear displacement, normal stress, mesh size, grain size, percent of open area, transverse rib, geotextile.

✉Corresponding author. E-mail: [jurgis.medzvieckas@vilniustech.lt](mailto:jurgis.medzvieckas@vilniustech.lt)

## 1. Introduction

Increasing the shear strength of sands using different techniques has been the focus of many researchers since the past. One of those techniques is specifically adding polymer fibers to sand or using geotextile and geogrid layers within soil mass (Lakirouhani et al., 2018; Albuja-Sánchez et al., 2023).

Geogrid is a type of material commonly used in civil engineering and construction projects. It is typically made of polymer materials, such as polyester or polypropylene, and is designed to reinforce soil or aggregate materials. Geogrids help to improve the strength and stability of the ground by distributing loads more evenly and reducing the potential for soil erosion. They are often used in applications such as road and railway construction, retaining walls, bridge abutments, embankments and slope stabilization. Geogrids are formed by a regular network of inte-

grally connected elements, while geogrid openings allow for interlocking with granular soils and other surrounding materials. Currently, several types of geogrids are commercially produced; for example, woven, welded or extruded geogrids. Also, according to the geometric shape of the openings, geogrids can be divided into three categories: uniaxial, biaxial, or triaxial. Also, from the point of view of flexibility, geogrids may be flexible or rigid.

Geogrids have a great impact on the stress-strain behavior of reinforced soil due to the confinement in the soil. As a result, reinforced soil structures have better stability than non-reinforced soils. Geogrids increase the shear strength of the soil and preventing the lateral expansion of the soil. Geogrid layers strengthen the soil mass due to their high resistance to tensile and shear forces. The better the bond and interlocking between the granular soil and

the geogrid, the better the performance of the geogrid in the soil mass. Two failure mechanisms are considered for the geogrid in the reinforced soil mass; pull-out failure and sliding along the geogrid-soil interface (Palmeria & Milligan, 1989). The load bearing capacity of reinforcement for pullout is measured using the pull-out test. This test can be done using a physical model in a small scale in the laboratory or a real scale in the field (Farrag et al., 1993). In the pullout test, a geogrid layer between two soil layers is pulled out by a horizontal force. The pullout resistance, which represents the degree of interlocking between the geogrid and the soil, is the maximum force required to pull the geogrid out of the soil mass.

By using the pullout test, many researchers have studied the interaction between the geogrid and the surrounding soil (Lopes & Ladeira, 1996; Ochiai et al., 1996; Chang et al., 2000; Sugimoto et al., 2001; Palmeira, 2004; Moraci & Giofrè, 2006; Moraci & Recalcati, 2006; Sieira et al., 2009; Palmeira, 2009; Horpibulsuk & Niramitkornburee, 2010; Ezzein & Bathurst, 2014; Chen et al., 2014; Prashanth et al., 2016; Cardile et al., 2017, 2021; Suksiripattanapong et al., 2020; Ferreira et al., 2020; Sharbaf & Ghafoori, 2021; Park et al., 2021; Alimohammadi et al., 2021).

The failure caused by sliding is highly dependent on the shear strength of the soil-geogrid interface, which can be evaluated using a large-scale direct shear test (Praveen & Kurre, 2021; Lakirouhani et al., 2023) or triaxial test (Skuodis et al., 2020). In the direct shear test, a geogrid layer is placed on the soil layer inside the lower shear box and at the interface between the two shear boxes. Then, under a constant normal stress applied to the specimen, a shear displacement or shear stress is applied to the lower shear box so that slip occurs along the interface. For each test, the shear stress versus shear displacement can be recorded and from this curve, the peak shear stress can be obtained as the shear strength of the sample under a certain normal stress. By repeating the test for three different normal stresses, it is possible to obtain the Mohr Coulomb failure envelope for the sample.

The decrease or increase in the shear strength of the soil-geogrid interface is shown using the  $\alpha$  parameter.  $\alpha$  is the ratio of the shear strength of the soil-geogrid interface to the shear strength of unreinforced soil (pure soil) and is referred to as the interface shear strength coefficient (Liu et al., 2009a; Indraratna et al., 2012; Sakleshpur et al., 2019). If  $\alpha$  is more than one from the results of direct shear tests, it indicates the positive effect of geogrid in the reinforced soil mass system, and if  $\alpha$  is less than one, it indicates the lack of sufficient interlocking between soil particles and geogrid (Indraratna et al., 2012; Sakleshpur et al., 2019). Friction between soil and geogrid depends on various factors, including particle size, granularity, moisture content, geogrid mesh size, and soil relative density. The studies conducted by Liu et al. (2009a) using a direct shear test apparatus on different polyester yarn geogrid reinforced soils showed that the  $\alpha$  ratio is between 0.89

and 1.01. Other tests carried out using polypropylene geogrid on fine sand and gravelly soils determined  $\alpha$  between 0.94 and 1.12 (Cancelli et al., 1992; Abu-Farsakh & Coronel, 2006; Abu-Farsakh et al., 2007). Xu et al. (2018) investigated the effect of scalping on the shear strength of crusher run using large-scale laboratory direct shear box tests and found that scalping significantly reduces the shear strength of the interface between the crusher run and the geogrid, so that in this case  $\alpha$  decreases and changes between 0.76 and 0.94, meanwhile, Sweta and Hussaini (2018) obtained the interface efficiency factor ( $\alpha$ ) between 0.83 and 1.06 by conducting large-scale direct shear tests on the railway ballast.

The interface shear strength of the soil against the geotextile or geomembrane is only caused by the friction between the soil and the geosynthetic, because the soil particles are not trapped inside the small openings of the geosynthetic, but the shear resistance at the geogrid-soil interface is more complex and depends on various factors. Part of the shear resistance is caused by the friction between the granular soil and the surfaces of the geogrid ribs. The second part of the shear strength is caused by the internal shear strength of the soil, within the open areas of the geogrid, and the third part of the shear resistance at the soil-geogrid interface is caused by the passive resistance between the soil and the transverse ribs of the geogrid (Berg et al., 2009; Liu et al., 2009b). The first and second mechanisms mentioned above have been evaluated by researchers such as Alfaro et al. (1995) and Tatlisoz et al. (1998). On the other hand, although so far, it has been determined in the pull out test that the contribution of the transverse ribs of the geogrid in the passive resistance of the soil-geogrid interface is significant (Jewell, 1990; Bergado et al., 1993; Palmeira, 2004), but the effect of the transverse ribs in the direct shear test is disputed. For instance, M. J. Lopes and M. L. Lopes (1999) stated that the contribution of passive resistance provided by the geogrid openings in the direct shear test is almost negligible, but Bergado et al. (1993) stated that the transverse ribs of the geogrid provide significant passive resistance at the geogrid-soil interface. The relative density of the soil samples also has a great effect on the shear resistance of the soil-geogrid interface, but because limited studies have been done in relation to the relative density, it is difficult to compare the results of different researchers. Mochizuki et al. (2023) investigated the shear zone in Japanese sands under CD conditions using an improved direct shear device (Mochizuki et al., 2021; Zhussupbekov et al., 2020). Using an artificial neural network and data sets obtained from a large-scale direct shear test, Hasan-zadehshooili et al. (2014) predicted the collapse settlements of sandy gravels.

As stated above, although various studies have been conducted on the shear strength of the soil-geogrid interface, however, there are still many uncertainties regarding the effect of the relative dry density of the soil and

the size of the geogrid apertures on the resistance of the soil-geogrids interface and the passive resistance of the transverse ribs. The purpose of this article is to investigate the effect of the relative dry density of granular soil and the size of the aperture of the geogrid on the resistance of the soil-geogrid interface. In this study, a series of large-scale direct shear tests are performed using two types of granular soil; sand and gravel, and 5 types of geogrids. Geogrids have the same material but different size of apertures. Direct shear tests using a type of geotextile are also performed and the results are compared with the results obtained for unreinforced sand and gravel samples. To investigate the effect of relative density, experiments have been performed for different relative densities.

## 2. Testing program, soils and geogrids properties

The experiments of this paper were carried out using a large-scale direct shear apparatus with a 30 cm × 30 cm × 15 cm shear box (Figure 1), so that the shearing area was 0.09 m<sup>2</sup>. As regulated in ASTM D5321 (ASTM International, 2021), to check the resistance of the soil-geosynthetic interface, the dimensions of the shear box should be at least 30 cm × 30 cm. Two different soils were used in the experiments, sand and gravel, Figure 2 shows their grain size distribution curves, while Table 1 shows their physical characteristics. The sand and gravel used are classified as SP and GP, respectively, according to the Unified Soil Classification System (USCS). In this study, 5 geogrids with the same material but different mesh sizes and one geotextile are used. Geogrids are denoted as Gr1, Gr2, Gr3, Gr4 and Gr5 respectively and the geotextile is named Gte. The specifications of geogrid Gr1, which is of ForTex 80/30™ type, are given in Table 2. ForTex geogrids™ is made PVC coated high tenacity polyester by knit woven technology. Geogrid Gr1 has a mesh size of 2.5 cm × 2.5 cm and other geogrids are produced by removing some of the longitudinal and transverse ribs of geogrid Gr1. Figure 3 schematically shows geogrids, in this figure the percent of open area of geogrids is also specified ( $\rho$ ),  $\rho$  is the ratio of the opening area to the total area of the geogrid. The geotextile used in the experiments is woven with a weight of 250 g/m<sup>2</sup>. For a better comparison of the results, the direct shear test with the same previous method and the same normal stress was also performed on pure sand and pure gravel. The soil used in the direct shear tests is compacted in three layers in the shear box, according to its dry unit weight. Sand compaction in the shear box is done using a standard proctor hammer at the optimum water content (12.60%) and gravel compaction is done using a plastic hammer at the optimum water content (0.8%).

This study attempts to show the effect of relative dry density ( $D_r$ ) on soil/geogrid interface resistance, so tests are carried out on sand samples for three different relative densities of 40%, 55% and 70%, but the tests of gravel samples are only done for a relative density of 70%.



Figure 1. Large scale direct shear test device

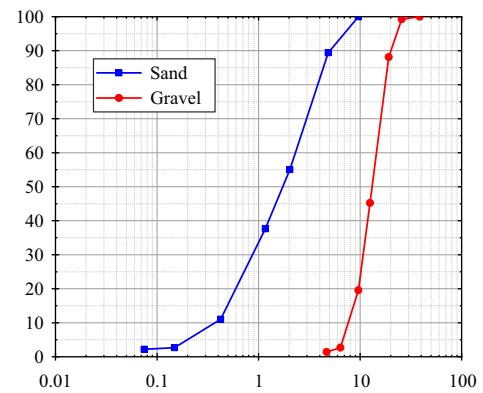


Figure 2. Aggregate gradation curves

Thus, for a certain relative density, the weight of each sample can be obtained according to Eqn (1):

$$D_r = \frac{\gamma_{d\max}(\gamma_d - \gamma_{d\min})}{\gamma_d(\gamma_{d\max} - \gamma_{d\min})} \times 100, \quad (1)$$

where  $D_r$  is the relative density,  $\gamma_{d\max}$  is dry unit weight in the densest condition (at a void ratio of  $e_{\min}$ ),  $\gamma_{d\min}$  is dry unit weight in the loosest condition (at a void ratio  $e_{\max}$ ) and  $\gamma_d$  is in situ dry unit weight at a void ratio of  $e$ .

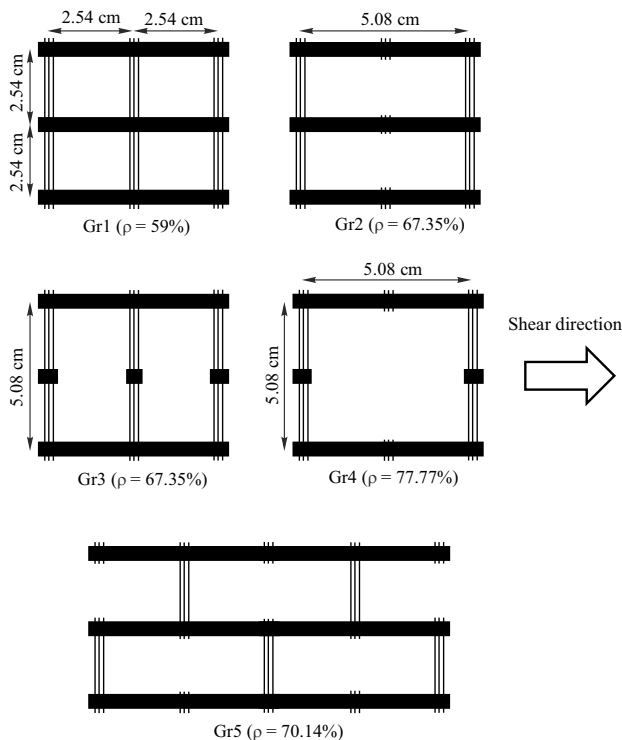
The geogrid or geotextile layer is spread on top of the lower shear box and fixed in place by special fasteners. Tests are performed under three normal stresses 100 kPa, 200 kPa and 300 kPa. After applying the vertical load, the sample is shear with a constant displacement rate at speed 1 mm/min (ASTM International, 2021). It should be noted that shear displacement is not applied until the vertical displacement reaches equilibrium. The shearing of the sample continues until the shear displacement reaches about 40 mm. During sample shearing, shear stress, shear displacement and vertical displacement of the sample are recorded and the peak (maximum) shear stress is considered as the shear strength of the sample. Figure 4 shows the gravel-geogrid, sand-geogrid and sand-geotextile interface on top of the lower shear box.

**Table 1.** Soils physical characteristics

Parameter	Symbol	Unit	Soil type	
			Sand	Gravel
Optimum moisture content	$\omega_{opt}$	%	12.6	0.8
Maximum dry unit weight	$\gamma_{d max}$	kg/m <sup>3</sup>	1870	1810
Minimum dry unit weight	$\gamma_{d min}$	kg/m <sup>3</sup>	1660	1570
Specific gravity	$G_s$	---	2.69	2.84
Coefficient of gradation	$C_c$	---	0.99	1.01
Uniformity coefficient	$C_u$	---	6.18	1.92
Diameter through which 10% of the total soil mass is passing	$D_{10}$	mm	0.39	7.67
Diameter through which 30% of the total soil mass is passing	$D_{30}$	mm	0.96	10.72
Diameter through which 50% of the total soil mass is passing	$D_{50}$	mm	1.76	13.23
Diameter through which 60% of the total soil mass is passing	$D_{60}$	mm	2.40	14.74
Classification (USCS)			SP	GP

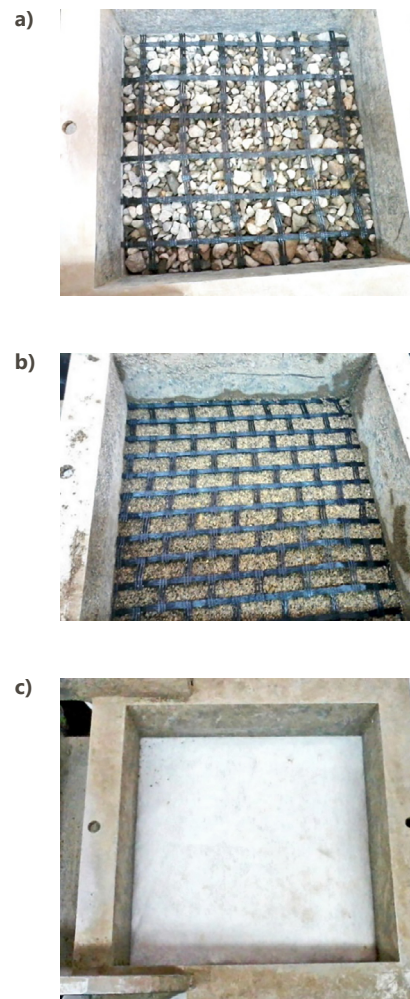
**Table 2.** Characteristics of ForTEX 80/30 Polyester Geogrids™

Specifications	Unit	Longitudinal Ribs	Transverse Ribs
Tensile strength	kN/m	80	30
Elongation at failure	%	15	15
Aperture size	mm	25.4	25.4

**Figure 3.** Geogrids with different mesh sizes relative to the shear direction

### 3. Results obtained for pure sand and gravel

In this section, the results of direct shear tests conducted on pure soil samples are presented. The results are given in Figures 5 to 8. Figures 5 to 7 show shear stress and vertical displacement versus shear displacement for pure sand

**Figure 4.** Reinforcement of samples with geogrid and geotextile: a – Gravel with geogrid Gr1; b – Sand with geogrid Gr5; c – Sand and geotextile

with different relative densities. As can be seen, the stress-strain curves have a peak and the peak stress increased with the increase of the normal stress. Also, by increasing the dry relative density, the strength of the samples increases. The displacement corresponding to the peak

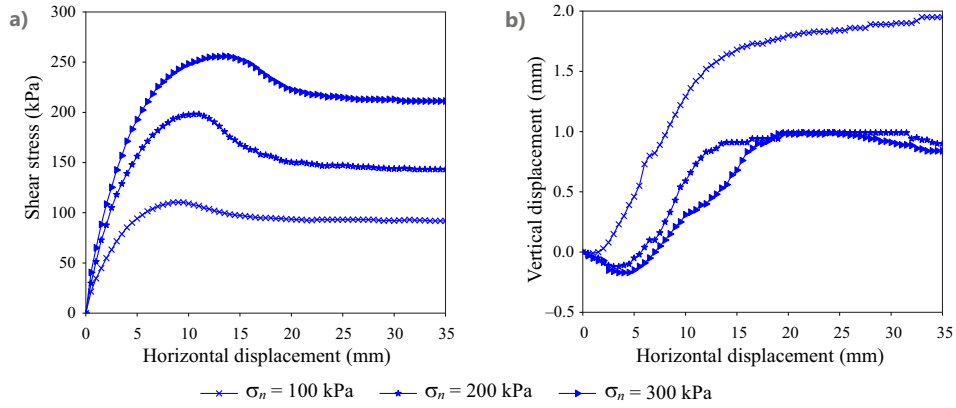


Figure 5. a – Shear stress-horizontal displacements; b – Vertical displacement-horizontal displacement, pure sand ( $D_r = 40\%$ )

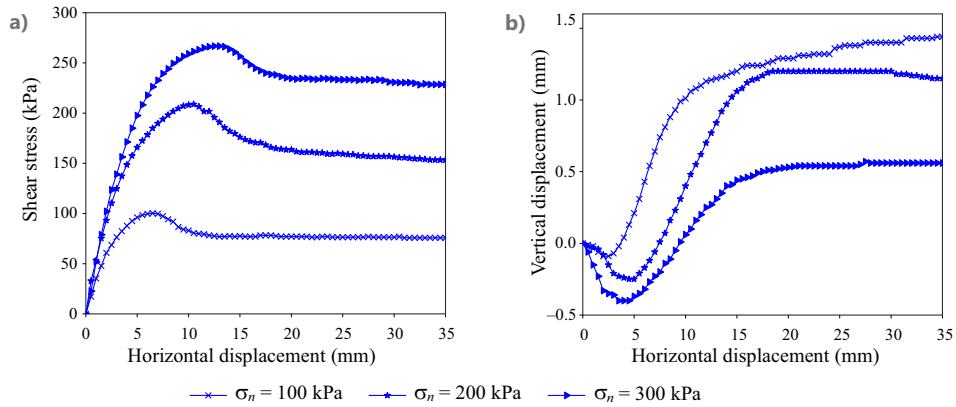


Figure 6. a – Shear stress-horizontal displacements; b – Vertical displacement-horizontal displacement, pure sand ( $D_r = 55\%$ )

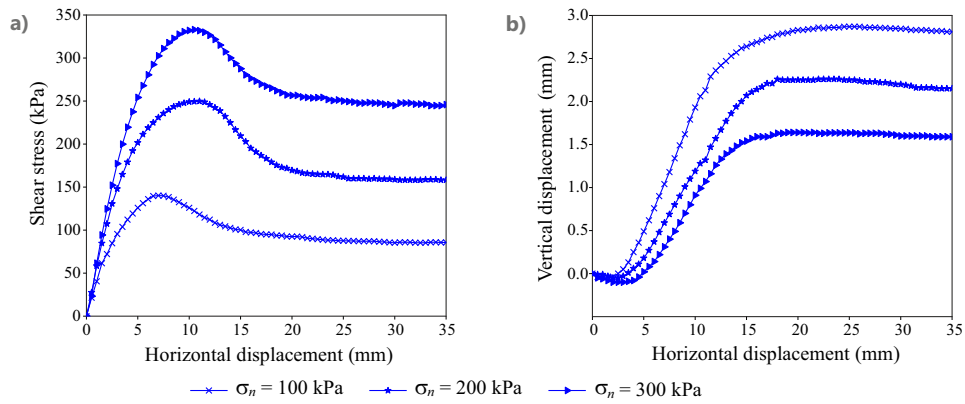


Figure 7. a – Shear stress-horizontal displacements; b – Vertical displacement-horizontal displacement, pure sand ( $D_r = 70\%$ )

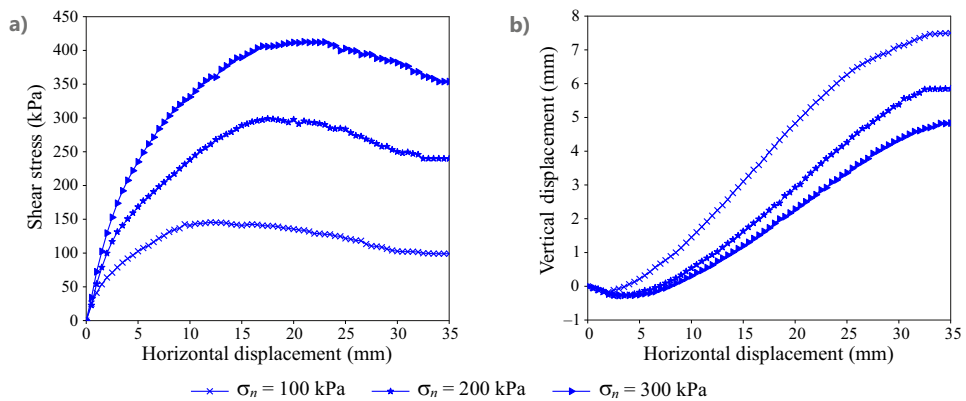


Figure 8. a – Shear stress-horizontal displacements; b – Vertical displacement-horizontal displacement, pure gravel ( $D_r = 70\%$ )

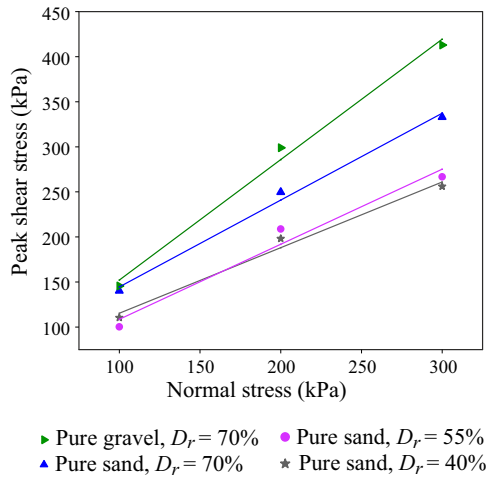


Figure 9. Peak shear stress versus normal stress

stress is between 8 mm and 14 mm and with the increase of the normal stress, the displacement at the location of peak stress has increased. The shearing behavior of gravel is different from that of sand, and in gravel samples, the maximum shear strength occurs at larger shear displacements (Figure 8). The shear strength of gravel samples is significantly higher than sand samples. The rate of reduction of shear stress against shear displacement is lower for gravel samples than for sand. In the figures, it can be seen that all the samples have a reduction in volume at first, and then they undergo dilation due to their high relative density. As the normal stress increases, the increase in the final vertical displacement of the sample decreases, and the increase in the vertical displacement of gravel samples is more than the sand sample. In Figure 9, the peak shear stress versus normal stress for each series of samples is given, also in this figure, the Mohr Coulomb shear failure envelope (best fitted straight line) for different relative densities is shown.

#### 4. Results obtained for the shear strength of the soil-geotextile interface

Figures 10 to 14 illustrate the results obtained for soil/geotextile interface strength and comparison with pure sand and pure gravel. In these figures, it can be seen that the shear behavior of the soil sample reinforced with geotextile is completely different from the shear behavior of pure sand or pure gravel.

First, the shear stress-shear displacement curves of the sand-geotextile interface have an initial peak, and then the shear behavior becomes strain hardening. Due to the lack of interlocking between sand particles on the shear surface, in some cases, the peak in the shear behavior of the sample reinforced with geotextile is not observed. Secondly, the peak shear strength of sand-geotextile is significantly lower than that of pure sand, although the residual strengths of the reinforced sand sample and pure sand approach each other (Figures 10 to 12). As well as, the shear stiffness of samples reinforced with geotextile (slope of initial portion of the shear stress/shear displacement curve) is lower than that of pure samples. The decrease in the shear stiffness of the sample is the result of the sand grains sliding on the surface of the geogrid. It can be seen that under normal stress 100 kPa, the residual strength of the sample reinforced with geotextile becomes the same as the residual strength of pure sand (Figures 11 to 13), but as the normal stress increases, the difference between the residual strengths increases. In the plots of vertical displacement versus shear displacement, it can be seen that initially the reinforced sand sample has a greater decrease in volume than pure sand, but in large horizontal displacements, its expansion is less than pure sand, in other words, the geogrid layer at the interface of two shear boxes causes less expansion of the sample during shearing. Similar behavior can be seen for reinforced gravel samples (Figure 13).

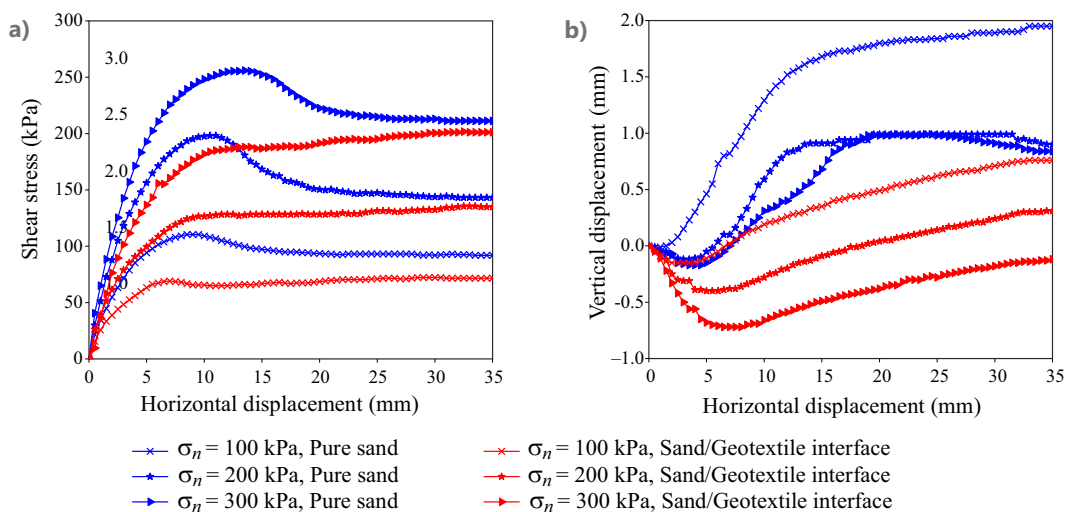


Figure 10. a – Shear stress-horizontal displacements; b – Vertical displacement-horizontal displacement. Comparison between pure sand and sand/geotextile interface ( $D_r = 40\%$ )

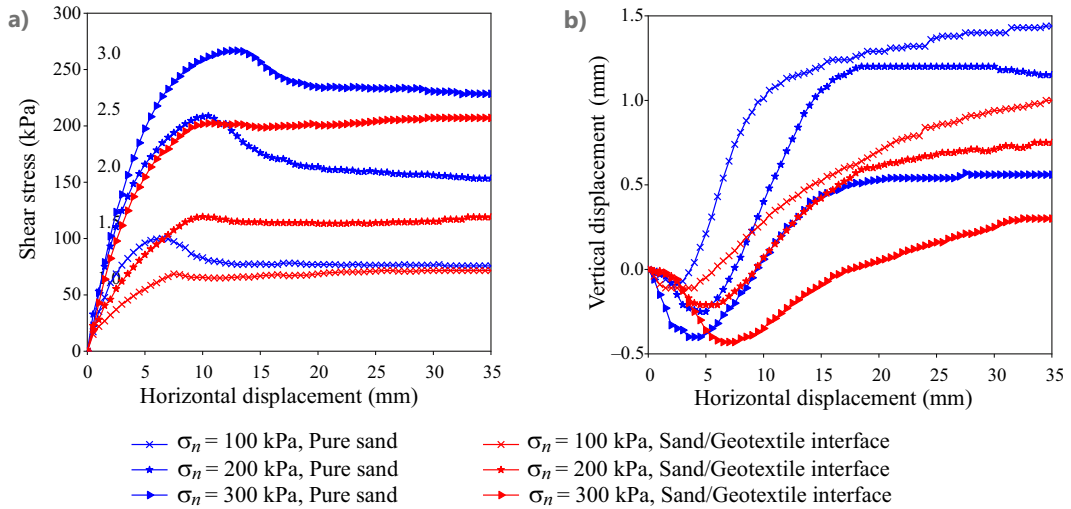


Figure 11. a – Shear stress-horizontal displacements; b – Vertical displacement-horizontal displacement. Comparison between pure sand and sand/geotextile interface ( $D_r = 55\%$ )

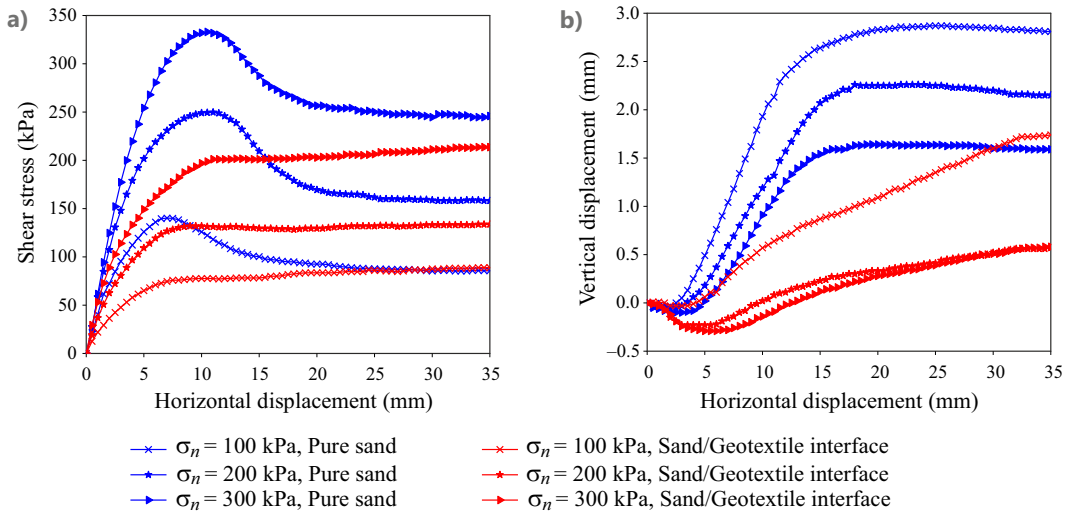


Figure 12. a – Shear stress-horizontal displacements; b – vertical displacement-horizontal displacement. Comparison between pure sand and sand/geotextile interface ( $D_r = 70\%$ )

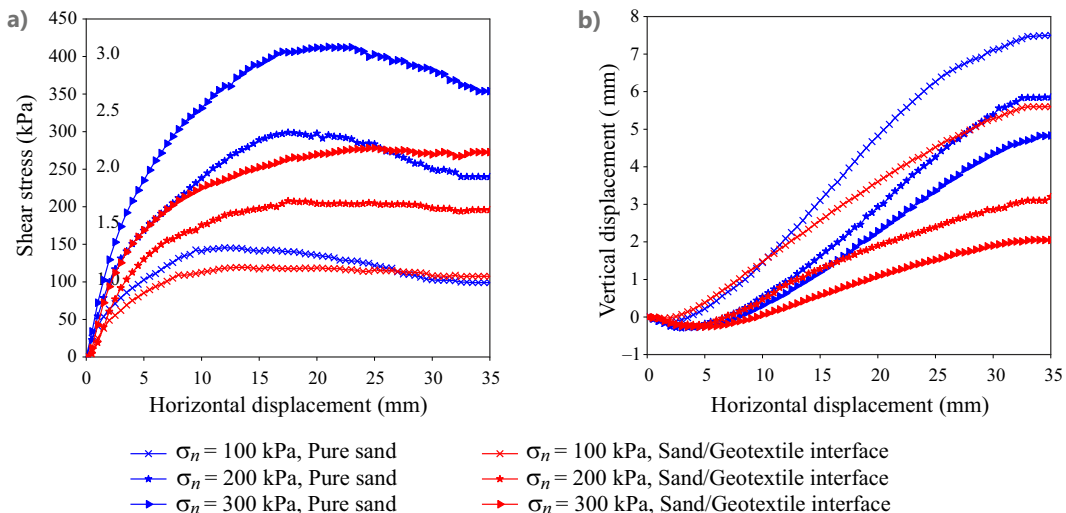


Figure 13. a – Shear stress-horizontal displacements; b – Vertical displacement-horizontal displacement. Comparison between pure gravel and gravel/geotextile interface ( $D_r = 70\%$ )

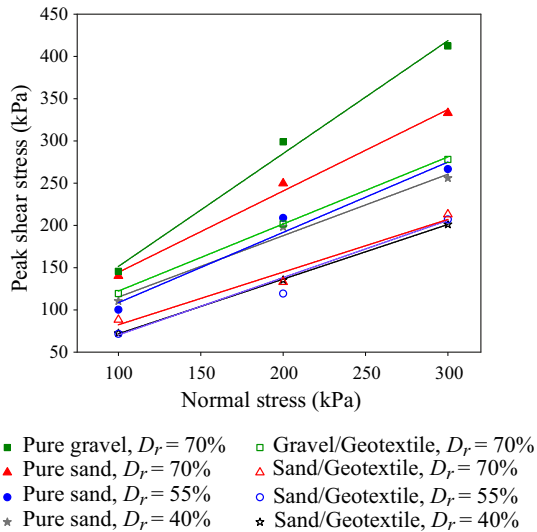


Figure 14. Peak shear stress versus normal stress

Figure 14 shows the peak shear stress versus normal stress, the highest strength is for pure gravel with a relative density 70%, followed by pure sand with a relative density of 70%, 55%, and 40%, respectively. Another result obtained from Figure 14 is that the difference in shear strength of sand samples reinforced with geotextile with different relative densities is insignificant, although it was seen in Figure 9 that pure sands with higher relative density had higher shear strength. But the resistance of the gravel/geotextile interface is higher than the shear resistance of the sand/geotextile interface with the same relative density, this indicates that the thickness of the shear zone, which affects the shear strength of the sample, increases with the increase in the grain size.

## 5. Results obtained for the shear strength of the soil-geogrid interface

Next, direct shear tests are performed on samples of granular soil reinforced with 5 geogrids with different mesh sizes, and the results obtained are compared with the previous results obtained on pure soil and soil reinforced with geotextile. The results of these tests are given in Figures 15 to 18. Figures 15 to 17 are respectively for sand with a relative density of 40%, 55% and 70%, and Figure 18 is for gravel with a relative density of 70%. In each of these figures, there are 5 sub-figures, each sub-figure shows the results obtained for one of the geogrids, and the name of each geogrid is indicated on the figure.

As can be seen, the shear stress-shear displacement behavior of sand-geogrid interface is different from the behavior of pure sand and sand-geotextile interface. In other words, the sand-geogrid interface undergoes yielding after the initial peak, while the yield shear stress is slightly lower than the peak stress. After that, the shear stress of the sand-geogrid interface increases slowly and approaches the pure sand peak shear stress in large shear

displacements. The shear displacement at yield stress is similar to the shear displacement at peak stress for pure sand. An important result obtained from the comparison made in this section is that, at the sand-geogrid interface, the shear resistance of the sand particles across the openings, as well as the resistance between the sand and the surfaces of the geogrid ribs, are active in small shear displacements; meanwhile, passive resistances of transverse ribs are activated in large shear displacements. Figures 15 to 17 illustrate that the highest shear strength is for pure sand and the lowest shear strength occurs at the sand-geotextile interface and the shear strength of the sand-geogrid interface is between these two values. The initial slope of the shear stress versus shear displacement curve, known as the shear stiffness, for the sand-geogrid interface is similar to that of pure sand, but the shear stiffness of the sand-geotextile interface is lower than them.

But for brevity, only a series of curves of vertical displacement versus shear displacement are given. Figure 19 shows vertical displacement versus shear displacement for pure sand, sand-geogrid Gr1 interface, and geotextile-reinforced sand. The vertical displacement versus shear displacement curves of the sand/geogrid interface are between the vertical displacement curves of pure sand and sand/geotextile. At first, the reduction in volume of geogrid-reinforced samples is more than that of pure sand and less than that of geotextile-reinforced sand, but then their dilation becomes greater than that of geotextile-reinforced sand and less than that of pure sand.

## 6. Discussion on the effect of geogrid aperture size using interface shear strength coefficient $\alpha$

In this section, using the shear strength coefficient of the interface that was mentioned earlier in the introduction, the effect of the passive resistance of the transverse ribs of the geogrid, the size of the opening of the geogrid and also the relative density on the strength of the reinforced samples is investigated. The shear strength coefficient of the interface is defined as in Tatlisoz et al. (1998):

$$\alpha = \frac{\tau_{\text{soil-Geosynthetic}}}{\tau_{\text{soil}}} \quad (2)$$

Interface shear strength coefficient is equal to the ratio of the maximum shear strength of the soil-geosynthetic interface to the maximum shear strength of pure sand/gravel.  $\alpha$  for all direct shear tests performed on sand and gravel samples reinforced with geotextile and geogrid and for normal stresses 100 kPa, 200 kPa and 300 kPa, and geogrids Gr1, Gr2, Gr3, Gr4 and Gr5 and different relative densities is obtained. The results are illustrated in Figures 20 and 21. Figure 20 shows  $\alpha$  values for different normal stresses and in Figure 21, the average  $\alpha$  for three normal stresses is given. Figure 20 is only for peak stress and Figure 21 is for both peak stress and yield stress.



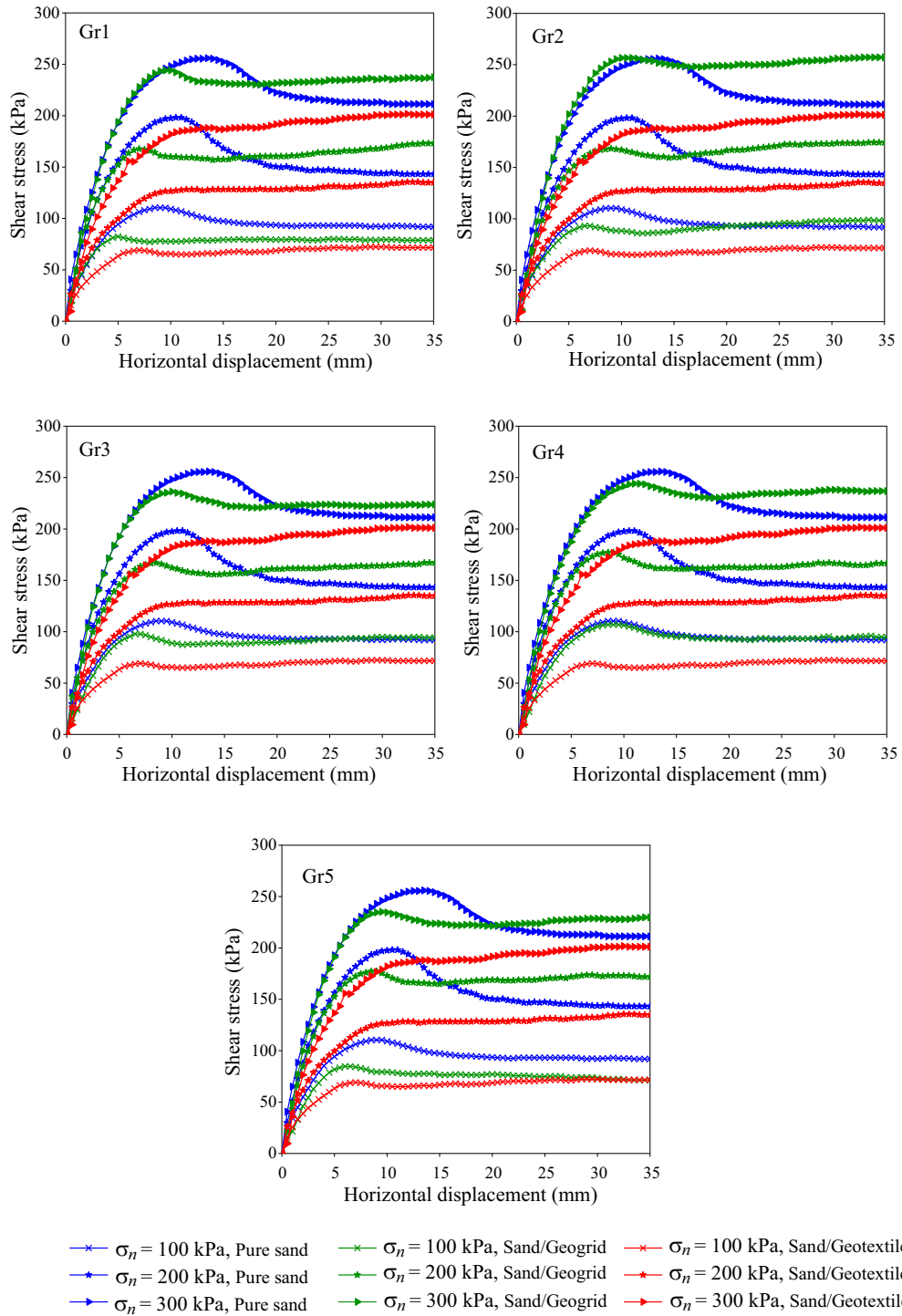


Figure 15. Shear stress versus horizontal displacements: pure sand, sand/geotextile, sand-geogrid ( $D_r = 40\%$ )

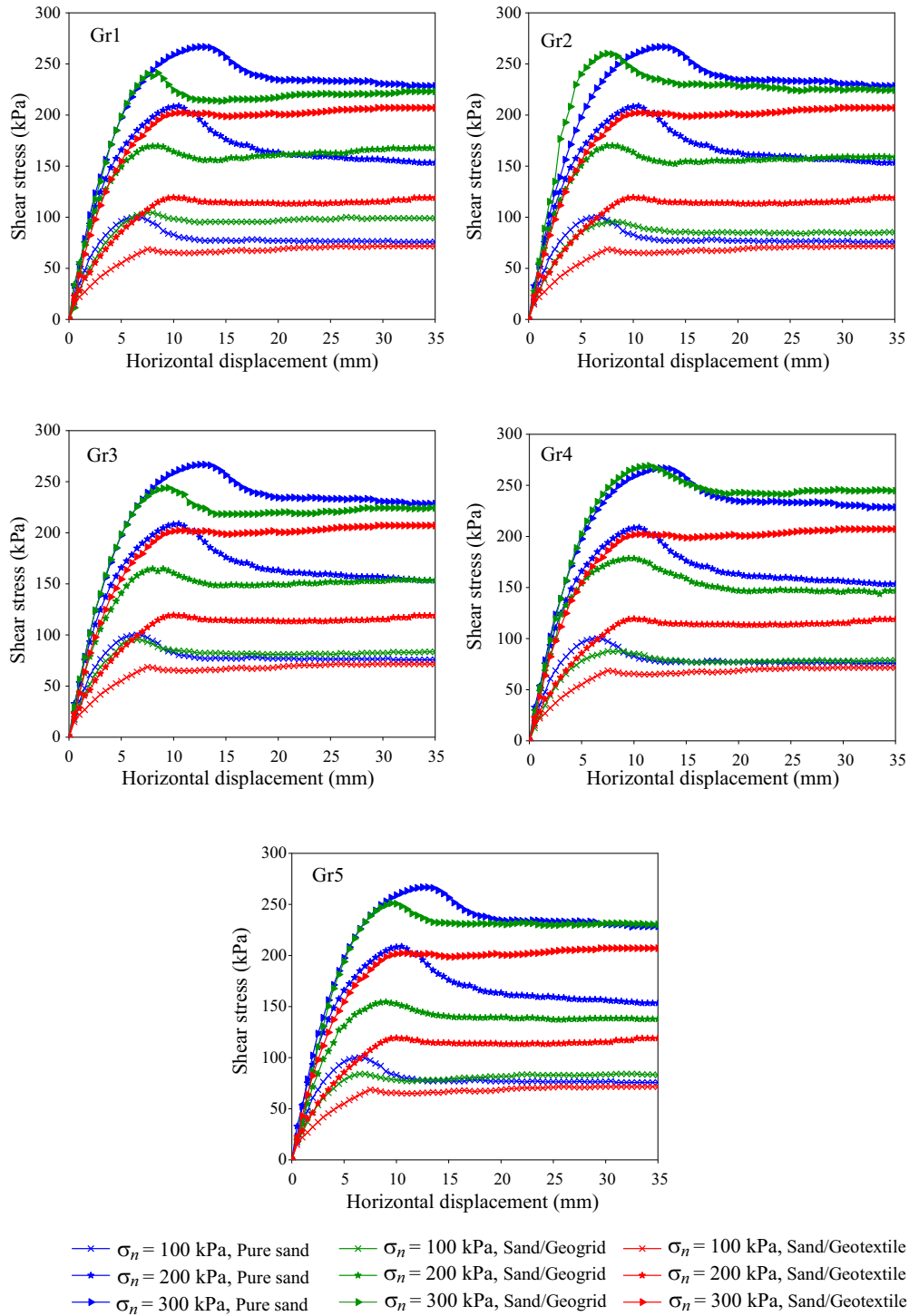


Figure 16. Shear stress versus horizontal displacements: pure sand, sand/geotextile, sand-geogrid ( $D_r = 55\%$ )

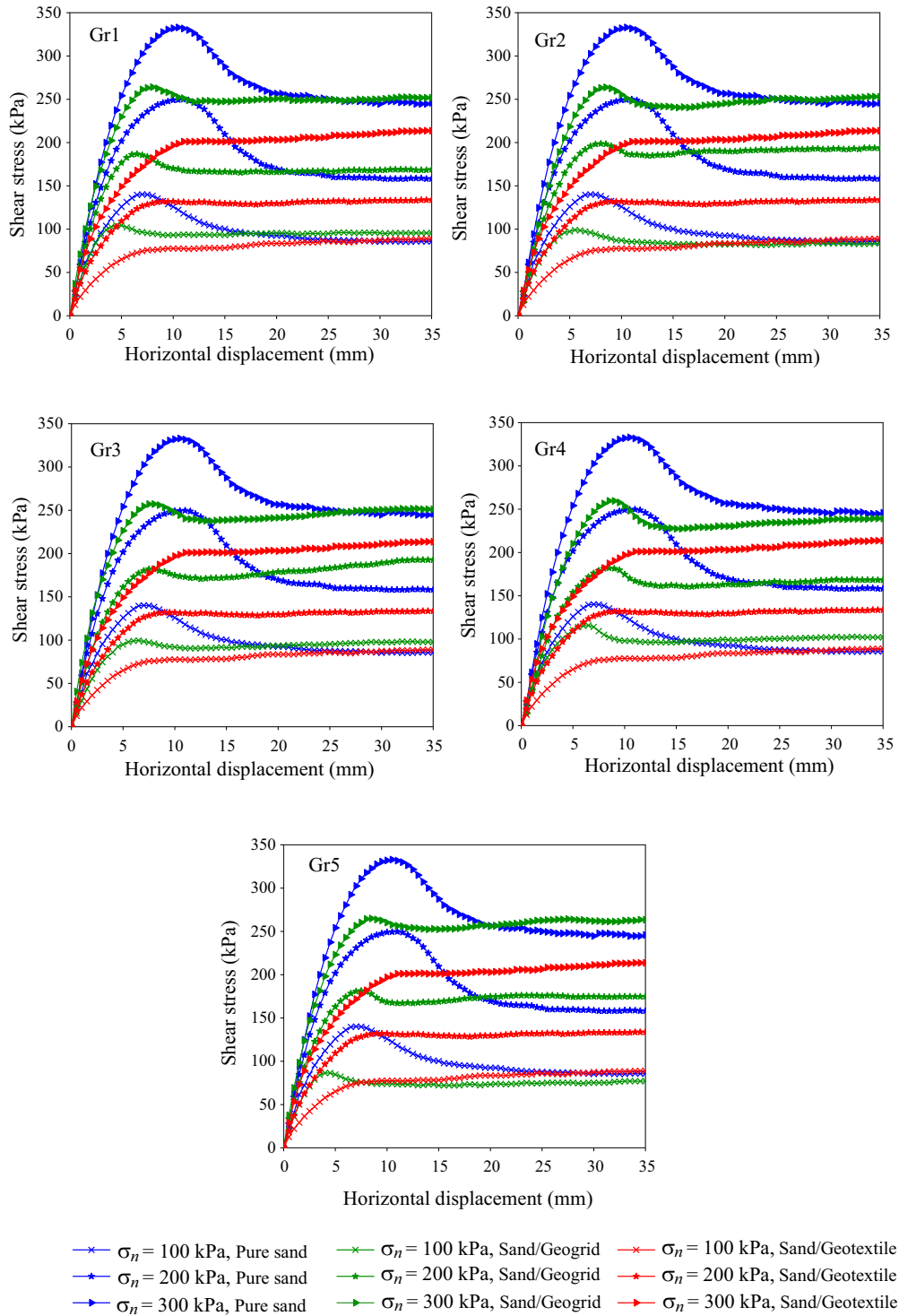


Figure 17. Shear stress versus horizontal displacements: pure sand, sand/geotextile, sand-geogrid ( $D_r = 70\%$ )

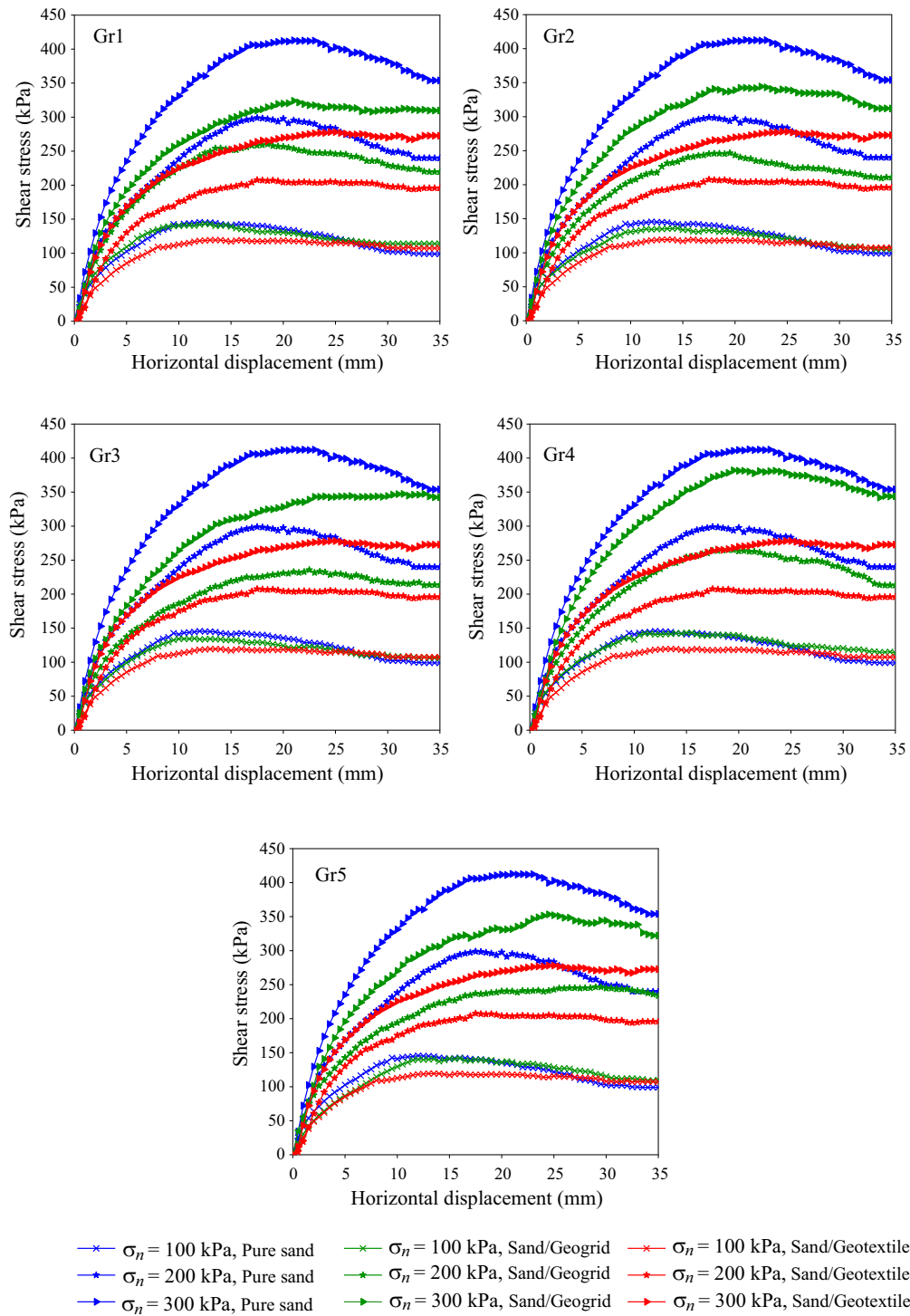


Figure 18. Shear stress versus horizontal displacements: pure gravel, gravel/geotextile, gravel-geogrid ( $D_r = 70\%$ )

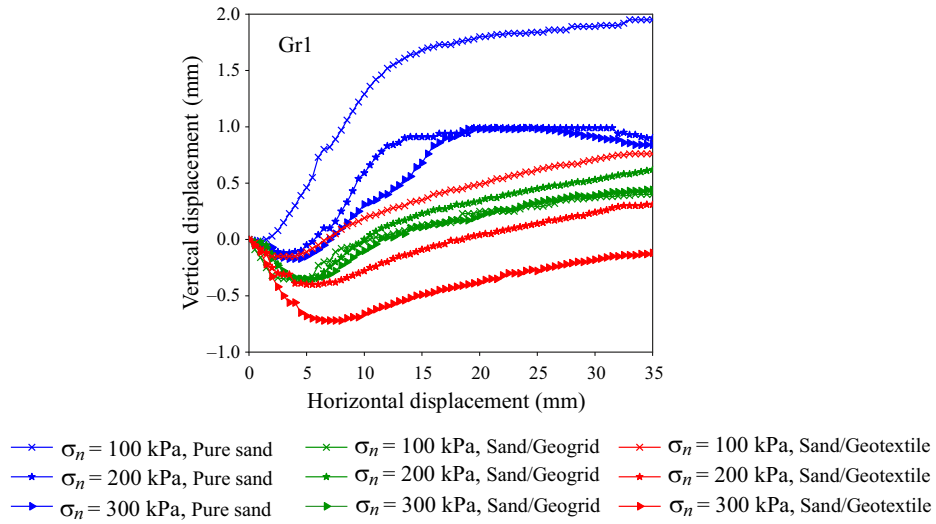


Figure 19. Vertical displacement versus horizontal displacement ( $D_r = 40\%$ )

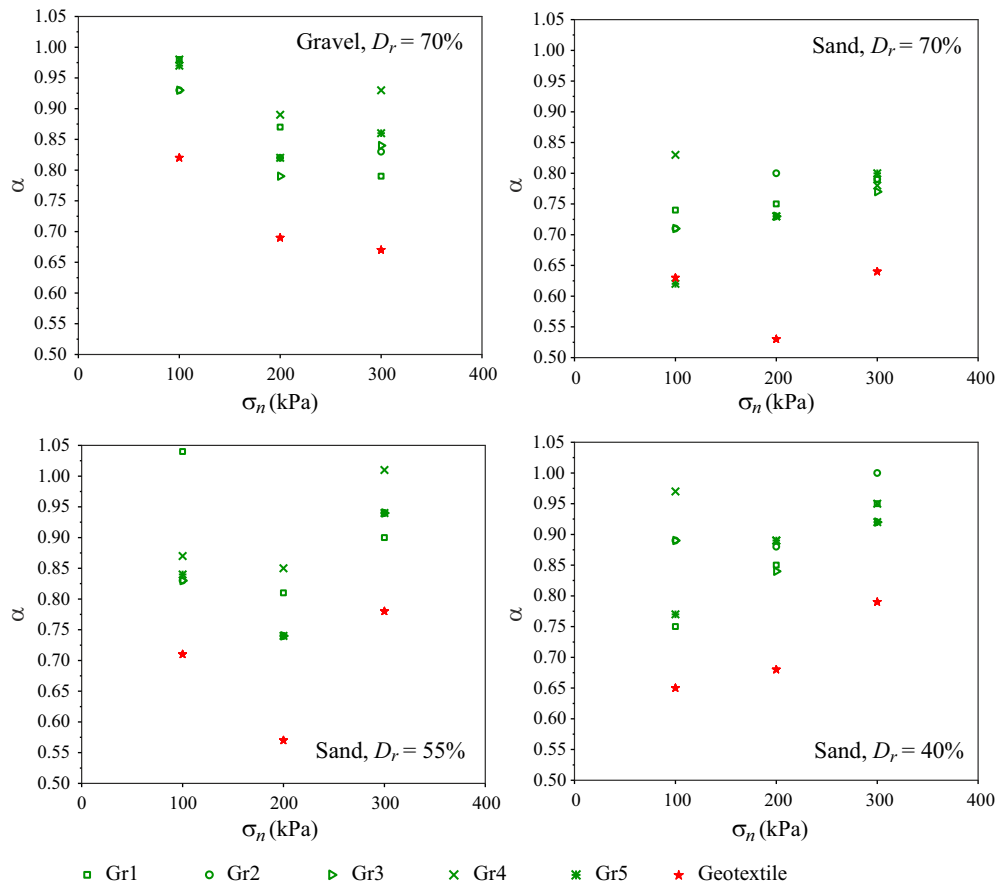
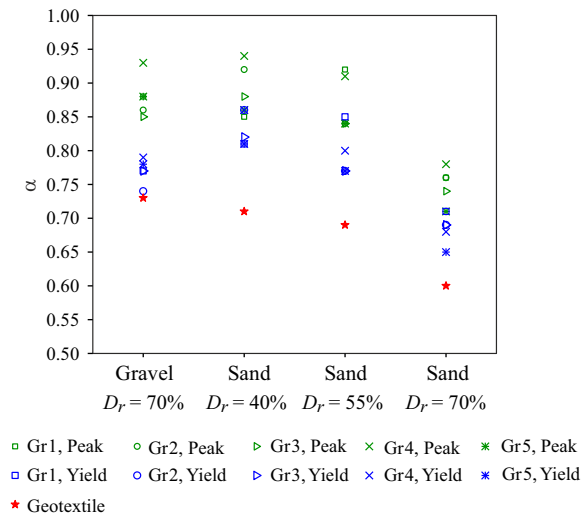


Figure 20. Interface shear strength coefficient versus normal stress, for samples with different relative densities

According to Figure 21, the average shear strength coefficient of the granular soil/geotextile interface is between 0.6 and 0.73. In other words, the lowest  $\alpha$  value at the soil-geotextile interface occurs for sand/geotextile interface with a relative density of  $D_r = 70\%$  under normal stress  $\sigma_n = 200$  kPa, in this case  $\alpha = 0.53$ , this means that in this case the shear strength of the sand/geotextile interface decreases to about 50% of the shear strength of pure

sand. The highest value of  $\alpha$  is obtained at the gravel/geotextile interface with a relative density of  $D_r = 70\%$  and under normal stress  $\sigma_n = 100$  kPa with a value of  $\alpha = 0.82$ . Similar values have been reported by other researchers studying the sand-geotextile interface, for instance, Liu et al. (2009b) found  $\alpha$  coefficients between 0.7 and 0.8 at the sand/geotextile interface.



**Figure 21.** Average interface shear strength coefficient for samples with different relative densities

The coefficient of shear strength,  $\alpha$ , obtained at the soil/geogrid interface is higher than the  $\alpha$  coefficient at the soil/geotextile interface under the same conditions. This is because the interlocking of soil particles above and below the geogrid is allowed within geogrid openings, and of course, the contribution of the transverse ribs of the geogrid to the shear resistance is also significant. But in these cases,  $\alpha$  is still less than 1, except for three cases in which  $\alpha$  becomes one or slightly more than one. An important result obtained from Figure 21 is that in sands, the resistance of the sand/geogrid interface or sand/geotextile interface decreases with increasing relative density, this result is valid for all geogrid types with different mesh sizes. In other words, the higher the relative density of the sand, or the denser it is, the greater the reduction in shear strength at the interface, or, the looser the sand, the less the shear strength of the sand/geogrid interface decreases compared to pure sand. This result shows the significant effect of shear zone on the shear strength of granular soil samples. Among the 5 types of geogrids, the largest value of the shear strength coefficient ( $\alpha$ ) was obtained at the interface between sand and geogrid Gr4. This is because, as seen in Figure 3, geogrid Gr4 has the largest mesh dimensions and the highest percent of open area ( $\rho$ ), therefore, the contribution of sand particle interlocking in the shear strength for this geogrid is more than other geogrids.

Figures 20 and 21 illustrate that as the dimensions of the geogrid mesh become larger, especially in the shear direction, the  $\alpha$  ratio increases. The largest  $\alpha$  coefficient is obtained for the sand/geogrid Gr4 interface, followed by the sand/geogrid Gr1 and sand/geogrid Gr2 interfaces, and the smallest  $\alpha$  coefficient is obtained for the sand/geogrid Gr3 and sand/geogrid Gr5 interface. The  $\alpha$  ratio at the interface between sand and geogrid Gr4 is 1.01, under normal stress  $\sigma_n = 300$  kPa, and at the interface between

sand and geogrid Gr1, under normal stress  $\sigma_n = 100$  kPa, it is 1.04 and at the interface between sand and geogrid Gr2, it is 1.00 under normal stress  $\sigma_n = 300$  kPa. The average shear strength coefficient is between 0.85 and 0.93 at the interface between gravel and geogrid, so that it is 0.93 at the interface between gravel and geogrid Gr4 and 0.85 at the interface between gravel and geogrid Gr3. The average coefficient of shear strength at the interface between gravel and geotextile is 0.73.

As mentioned earlier in the introduction, the resistance of the granular soil/geogrid interface is caused by three components: a) internal shear resistance of sand particles within the open areas of the geogrid, b) shear resistance between the sand and the surfaces of the geogrid ribs, and c) passive resistance between the soil and the transverse ribs of the geogrid. The results of the experiments conducted in this article showed that the largest contribution to the shear resistance of the sand/geogrid interface is caused by the first component, i.e., the internal shear resistance of the sand particles within the open areas of the geogrid. In Figure 21, it can also be seen that the  $\alpha$  obtained based on the yield stress is slightly lower than the  $\alpha$  obtained from the peak stress, because as seen in the shear stress-shear displacement curves, the yield stress was lower than the peak stress. The values obtained for  $\alpha$  are close to the values obtained by other researchers. For example, Liu et al. (2009a) conducted conventional direct shear tests and found that  $\alpha$  at the interface between Ottawa sand and woven polyester yarn geogrid was in the range of 0.89 to 1.01. Or in another case, Cancelli et al. (1992) obtained the shear resistance coefficient between 1.04 and 1.12 at the interface of fine-grained sand with polypropylene and high-density polyethylene geogrids. While Abu-Farsakh et al. (2007) obtained  $\alpha$  coefficient between 0.9 and 1.05 at the sand/polyethylene geogrid interface and for different moisture contents of the samples. The shear strength coefficient at the interface between crusher run and geogrid is greatly reduced and is between 0.76 and 0.94 (Xu et al., 2018), while at the interface between railway ballast and geogrid it is between 0.86 and 1.06 (Sweta & Hussaini, 2018). In short, the shear strength coefficient at the granular soil/geogrid interface depends on various parameters such as geogrid mesh size, geogrid transverse rib spacing, geogrid thickness, sand grading, sample moisture content, and test conditions.

## 7. Conclusions

This article presented the results of direct shear tests performed on sand and gravel samples reinforced with geogrid and geotextile. The focus of this article has been on the effect of the size of the geogrid openings and the relative density of the samples on the shear strength of the interface, as well as the investigation of the shear behavior of the reinforced samples. According to the results obtained:

1. The shear behavior of sand samples reinforced with geogrid is different from the shear behavior of sand samples reinforced with geotextile and pure sand. In this way, the shear stress-displacement curve for pure sand samples has a peak, and due to the complete interlocking between the sand particles on the shear surface, the difference between the peak stress and the residual stress is relatively large. However, in samples reinforced with geogrid, part of the interlocking between soil particles is removed due to the longitudinal and transverse ribs of the geogrid, and for this reason their peak strength is lower than that of pure sand. In the curve of shear stress versus shear displacement for sand reinforced with geogrid, the yield point is observed after the peak stress. Geotextile-reinforced sand samples do not have interlocking at the interface, consequently, the resistance of these samples is lower than pure sand samples and sand samples reinforced with geogrid.
2. The shear stiffness of pure sand is higher than sand reinforced with geogrid, and the shear stiffness of sand reinforced with geogrid is higher than sand reinforced with geotextile.
3. The average shear strength coefficient for sand and gravel samples reinforced with geotextile, for different relative densities, is between 0.6 and 0.73, while its lowest value is 0.53, this means that in samples reinforced with geotextiles, the shear resistance of the interface decreases to about 50% of the shear resistance of pure sand.
4. The average shear strength coefficient of sand and gravel samples reinforced with geogrid for different normal stresses and different relative densities is between 0.72 and 0.94. As the relative density increases, the interface shear strength coefficient decreases, this means that the denser the sand, the more the shear strength of the sand/geogrid interface decreases.
5. The shear resistance of the interface is caused by three components: a) interlocking of sand particles within geogrid openings, b) friction between the surfaces of geogrid ribs and sand, and c) passive resistance of transverse ribs. Hardening behavior after yielding in sand reinforced with geogrid shows that passive resistance of transverse ribs is activated in large shear deformations.
6. By increasing the size of the geogrid mesh, the interface shear strength coefficient increases. By increasing the size of the geogrid mesh, the interlocking of particles within the openings of the geogrid increases and the shear strength of the sample increases, consequently, the contribution of the particles interlocking in the shear strength of the sample is significant. According to the obtained results, the highest shear strength coefficient was obtained for the sand/geogrid Gr4 interface, the geogrid Gr4 has the highest percent of open area.

## References

- Abu-Farsakh, M. Y., & Coronel, J. (2006). Characterization of cohesive soil–geosynthetic interaction from large direct shear test. In *85th Transportation Research Board Annual Meeting*, Washington, D.C., USA.
- Abu-Farsakh, M., Coronel, J., & Tao, M. (2007). Effect of soil moisture content and dry density on cohesive soil–geosynthetic interactions using large direct shear tests. *Journal of Materials in Civil Engineering*, 19(7), 540–549.  
[https://doi.org/10.1061/\(ASCE\)0899-1561\(2007\)19:7\(540\)](https://doi.org/10.1061/(ASCE)0899-1561(2007)19:7(540))
- Albuja-Sánchez, J., Córdor, L., Oñate, K., Ruiz, S., & Lal, D. (2023). Influence of geogrid arrangement on the bearing capacity of a granular soil on physical models and its comparison to theoretical equations. *SN Applied Sciences*, 5(9), Article 250.  
<https://doi.org/10.1007/s42452-023-05474-w>
- Alfaro, M. C., Miura, N., & Bergado, D. T. (1995). Soil-geogrid reinforcement interaction by pullout and direct shear tests. *Geotechnical Testing Journal*, 18(2), 157–167.  
<https://doi.org/10.1520/GTJ10319J>
- Alimohammadi, H., Zheng, J., Schaefer, V. R., Siekmeier, J., & Velasquez, R. (2021). Evaluation of geogrid reinforcement of flexible pavement performance: A review of large-scale laboratory studies. *Transportation Geotechnics*, 27, Article 100471.  
<https://doi.org/10.1016/j.trgeo.2020.100471>
- ASTM International. (2021). *Standard test method for determining the shear strength of soil–geosynthetic and geosynthetic–geosynthetic interfaces by direct shear* (ASTM D5321). West Conshohocken, PA. <https://www.astm.org/d5321-12.html>
- Berg, R. R., Christopher, B. R., & Samtani, N. C. (2009). *Design of mechanically stabilized earth walls and reinforced soil slopes* (Volume I). Federal Highway Administration, United States.
- Bergado, D. T., Chai, J. C., Abiera, H. O., Alfaro, M. C., & Balasubramaniam, A. S. (1993). Interaction between cohesive-frictional soil and various grid reinforcements. *Geotextiles and Geomembranes*, 12(4), 327–349.  
[https://doi.org/10.1016/0266-1144\(93\)90008-C](https://doi.org/10.1016/0266-1144(93)90008-C)
- Cancelli, A., Rimoldi, P., & Togni, S. (1992). Frictional characteristics of geogrids by means of direct shear and pull-out tests. In *Proceedings of the International Symposium on Earth Reinforcement Practice* (Vol. 1, pp. 29–34), Kyushu, Japan.
- Cardile, G., Giofrè, D., Moraci, N., & Calvarano, L. S. (2017). Modelling interference between the geogrid bearing members under pullout loading conditions. *Geotextiles and Geomembranes*, 45(3), 169–177.  
<https://doi.org/10.1016/j.geotexmem.2017.01.008>
- Cardile, G., Pisano, M., Recalcati, P., & Moraci, N. (2021). A new apparatus for the study of pullout behaviour of soil-geosynthetic interfaces under sustained load over time. *Geotextiles and Geomembranes*, 49(6), 1519–1528.  
<https://doi.org/10.1016/j.geotexmem.2021.07.001>
- Chang, D.-T., Chang, F. C., Yang, G. S., & Yan, C. Y. (2000). The influence factors study for geogrid pullout test. In P. E. Stevenson (Ed.), *Grips, clamps, clamping techniques, and strain measurement for testing of geosynthetics* (Vol. STP1379-EB). ASTM International. <https://doi.org/10.1520/STP13477S>
- Chen, C., McDowell, G. R., & Thom, N. H. (2014). Investigating geogrid-reinforced ballast: Experimental pull-out tests and discrete element modelling. *Soils and Foundations*, 54(1), 1–11.  
<https://doi.org/10.1016/j.sandf.2013.12.001>
- Etzein, F. M., & Bathurst, R. J. (2014). A new approach to evaluate soil-geosynthetic interaction using a novel pullout test appa-

- ratus and transparent granular soil. *Geotextiles and Geomembranes*, 42(3), 246–255.  
<https://doi.org/10.1016/j.geotextmem.2014.04.003>
- Farrag, K., Acar, Y. B., & Juran, I. (1993). Pull-out resistance of geogrid reinforcements. *Geotextiles and Geomembranes*, 12(2), 133–159. [https://doi.org/10.1016/0266-1144\(93\)90003-7](https://doi.org/10.1016/0266-1144(93)90003-7)
- Ferreira, F. B., Vieira, C. S., & Lopes, M. d. L. (2020). Pullout behavior of different geosynthetics – Influence of soil density and moisture content. *Frontiers in Built Environment*, 6.  
<https://doi.org/10.3389/fbuil.2020.00012>
- Hasanzadehshooili, H., Mahinroosta, R., Lakirouhani, A., & Oshtaghi, V. (2014). Using artificial neural network (ANN) in prediction of collapse settlements of sandy gravels. *Arabian Journal of Geosciences*, 7(6), 2303–2314.  
<https://doi.org/10.1007/s12517-013-0858-9>
- Horpibulsuk, S., & Niramitkornburee, A. (2010). Pullout resistance of bearing reinforcement embedded in sand. *Soils and Foundations*, 50(2), 215–226. <https://doi.org/10.3208/sandf.50.215>
- Indraratna, B., Karimullah Hussaini, S. K., & Vinod, J. S. (2012). On the shear behavior of ballast-geosynthetic interfaces. *Geotechnical Testing Journal*, 35(2), 305–312.  
<https://doi.org/10.1520/GTJ103317>
- Jewell, R. A. (1990). Reinforcement bond capacity. *Géotechnique*, 40(3), 513–518. <https://doi.org/10.1680/geot.1990.40.3.513>
- Lakirouhani, A., Bahrehdar, M., & Hosseini, S. M. (2018). Investigation about shear behavior of sand reinforced with geotextile with emphasis on shear zone. *Sharif Journal of Civil Engineering*, 34.2(2.1), 99–108. <https://doi.org/10.24200/j30.2018.1345>
- Lakirouhani, A., Mousakhani, F., & Moazzami, A. (2023). Investigating the effect of particle size, granulation and concrete block on the behavior and shear strength of granular soils, with emphasis on the shear zone. *Road*, 37(117), 213–230.  
<https://doi.org/10.22034/road.2023.379498.2130>
- Liu, C.-N., Ho, Y.-H., & Huang, J.-W. (2009a). Large scale direct shear tests of soil/PET-yarn geogrid interfaces. *Geotextiles and Geomembranes*, 27(1), 19–30.  
<https://doi.org/10.1016/j.geotextmem.2008.03.002>
- Liu, C.-N., Zornberg J. G., Chen, T.-C., Ho, Y.-H., & Lin, B.-H. (2009b). Behavior of geogrid-sand interface in direct shear mode. *Journal of Geotechnical and Geoenvironmental Engineering*, 135(12), 1863–1871.  
[https://doi.org/10.1061/\(ASCE\)GT.1943-5606.0000150](https://doi.org/10.1061/(ASCE)GT.1943-5606.0000150)
- Lopes, M. L., & Ladeira, M. (1996). Influence of the confinement, soil density and displacement rate on soil-geogrid interaction. *Geotextiles and Geomembranes*, 14(10), 543–554.  
[https://doi.org/10.1016/S0266-1144\(97\)83184-6](https://doi.org/10.1016/S0266-1144(97)83184-6)
- Lopes, M. J., & Lopes, M. L. (1999). Soil-geosynthetic interaction – Influence of soil particle size and geosynthetic structure. *Geosynthetics International*, 6(4), 261–282.  
<https://doi.org/10.1680/gein.6.0153>
- Mochizuki, A., Zhussupbekov, A. Z., Fujisawa, J., Tanyrberganova, G., & Tulebekova, A. (2021). Strength anisotropy of compacted sandy material. *Soil Mechanics and Foundation Engineering*, 57(6), 480–490.  
<https://doi.org/10.1007/s11204-021-09696-1>
- Mochizuki, A., Zhussupbekov, A., Zharkenov, Y., Akhazhanov, S. (2023). Strength ellipses of induced anisotropy for a compacted sandy material. In A. Zhussupbekov, S. Sarsembayeva, & V. N. Kaliakin (Eds.), *Smart geotechnics for smart societies* (pp. 291–299). CRC Press.  
<https://doi.org/10.1007/s11204-021-09696-1>
- Moraci, N., & Giofrè, D. (2006). A simple method to evaluate the pullout resistance of extruded geogrids embedded in a compacted granular soil. *Geotextiles and Geomembranes*, 24(2), 116–128. <https://doi.org/10.1016/j.geotextmem.2005.11.001>
- Moraci, N., & Recalcati, P. (2006). Factors affecting the pullout behaviour of extruded geogrids embedded in a compacted granular soil. *Geotextiles and Geomembranes*, 24(4), 220–242.  
<https://doi.org/10.1016/j.geotextmem.2006.03.001>
- Ochiai, H., Otani, J., Hayashic, S., & Hirai, T. (1996). The pull-out resistance of geogrids in reinforced soil. *Geotextiles and Geomembranes*, 14(1), 19–42.  
[https://doi.org/10.1016/0266-1144\(96\)00027-1](https://doi.org/10.1016/0266-1144(96)00027-1)
- Palmeira, E. M. (2004). Bearing force mobilisation in pull-out tests on geogrids. *Geotextiles and Geomembranes*, 22(6), 481–509.  
<https://doi.org/10.1016/j.geotextmem.2004.03.007>
- Palmeira, E. M. (2009). Soil-geosynthetic interaction: Modelling and analysis. *Geotextiles and Geomembranes*, 27(5), 368–390.  
<https://doi.org/10.1016/j.geotextmem.2009.03.003>
- Palmeria, E. M., & Milligan, G. W. E. (1989). Scale and other factors affecting the results of pull-out tests of grids buried in sand. *Géotechnique*, 39(3), 511–542.  
<https://doi.org/10.1680/geot.1989.39.3.511>
- Park, K., Kim, D., Park, J., & Na, H. (2021). The determination of pullout parameters for sand with a geogrid. *Applied Sciences*, 11(1), Article 355. <https://doi.org/10.3390/app11010355>
- Prashanth, V., Murali Krishna, A., & Dash, S. K. (2016). Pullout tests using modified direct shear test setup for measuring soil-geosynthetic interaction parameters. *International Journal of Geosynthetics and Ground Engineering*, 2(2), Article 10.  
<https://doi.org/10.1007/s40891-016-0050-x>
- Praveen, G. V., & Kurre, P. (2021). Large direct shear testing to evaluate the interaction behaviour of murrum soil and geosynthetics for the reinforced soil construction. *Materials Today: Proceedings*, 39, 500–503.  
<https://doi.org/10.1016/j.matpr.2020.08.229>
- Sakleshpur, V. A., Prezzi, M., Salgado, R., Siddiki, N. Z., & Choi, Y. S. (2019). Large-scale direct shear testing of geogrid-reinforced aggregate base over weak subgrade. *International Journal of Pavement Engineering*, 20(6), 649–658.  
<https://doi.org/10.1080/10298436.2017.1321419>
- Sharbaf, M., & Ghafoori, N. (2021). Laboratory evaluation of geogrid-reinforced flexible pavements. *Transportation Engineering*, 4, Article 100070.  
<https://doi.org/10.1016/j.treng.2021.100070>
- Sieira, A. C. C. F., Gerscovich, D. M. S., & Sayão, A. S. F. J. (2009). Displacement and load transfer mechanisms of geogrids under pullout condition. *Geotextiles and Geomembranes*, 27(4), 241–253. <https://doi.org/10.1016/j.geotextmem.2008.11.012>
- Skuodis, Š., Dirgėlienė, N., & Medzvieckas, J. (2020). Using triaxial tests to determine the shearing strength of geogrid-reinforced sand. *Studia Geotechnica et Mechanica*, 42, 341–354.  
<https://doi.org/10.2478/sgem-2020-0005>
- Sugimoto, M., Alagiyawanna, A. M. N., & Kadoguchi, K. (2001). Influence of rigid and flexible face on geogrid pullout tests. *Geotextiles and Geomembranes*, 19(5), 257–277.  
[https://doi.org/10.1016/S0266-1144\(01\)00011-5](https://doi.org/10.1016/S0266-1144(01)00011-5)
- Suksiripattanapong, C., Horpibulsuk, S., Udomchai, A., Arulrajah, A., & Tangsutthinnon, T. (2020). Pullout resistance mechanism of bearing reinforcement embedded in coarse-grained soils: Laboratory and field investigations. *Transportation Geotechnics*, 22, Article 100297. <https://doi.org/10.1016/j.trgeo.2019.100297>



- Sweta, K., & Hussaini, S. K. K. (2018). Effect of shearing rate on the behavior of geogrid-reinforced railroad ballast under direct shear conditions. *Geotextiles and Geomembranes*, 46(3), 251–256. <https://doi.org/10.1016/j.geotexmem.2017.12.001>
- Tatliso, N., Edil, T. B., & Benson, C. H. (1998). Interaction between reinforcing geosynthetics and soil-tire chip mixtures. *Journal of Geotechnical and Geoenvironmental Engineering*, 124(11), 1109–1119. [https://doi.org/10.1061/\(ASCE\)1090-0241\(1998\)124:11\(1109\)](https://doi.org/10.1061/(ASCE)1090-0241(1998)124:11(1109))
- Xu, Y., Williams, D. J., Serati, M., & Vangsness, T. (2018). Effects of scalping on direct shear strength of crusher run and crusher run/geogrid interface. *Journal of Materials in Civil Engineering*, 30(9), Article 04018206. [https://doi.org/10.1061/\(ASCE\)MT.1943-5533.0002411](https://doi.org/10.1061/(ASCE)MT.1943-5533.0002411)
- Zhussupbekov, A., Tulebekova, A., Zhumadilov, I., & Zhankina, A. (2020). *Tests of soils on triaxial device*. KEM. <https://doi.org/10.4028/www.scientific.net/kem.857.228>